Core Loss Model for Switched Reluctance Motor in Electric Vehicles

[1]J.Kartigeyan and [2]M.Ramaswamy,
[1] Research Scholar, [2]Professor
[1,2]Electrical Engineering,
[1,2]Annamalai University, Chidambaram, India

Abstract : The paper attempts to evolve a model for determining the core loss of a switched reluctance motor (SRM), widely used as a drive for propulsion in electric vehicles (EV). The core loss forges to be one of the key factors in deciding the performance of the drive motor and requires extensive considerations to minimize it. The SRM offers promising characteristics to be suitable for the propulsion of a vehicle owing to its outstanding merits and use of steel lamination as the core material. The study involves the use of 2D-FEM analysis on a SRM with non-oriented electrical steel possibilities and brings out a strong correlation between the material flux density and permeability. The results relate the variation of motor core loss for different materials and exhibit the effect on core loss. The model manifests an empirical approach to the calculation of core loss besides establishing the strong relationship among the parameters of the magnetic material.

IndexTerms **- Core loss, FEM, non-oriented steels, SRM, time stepped 2D analysis.**

I. INTRODUCTION

The electric motor systems appear to use around 70% of the power demand from the industries [1] to support the emerging automated environment. However the energy scarce scenario and clean energy enforcements augur an efficient use of electric energy in the motor systems. The improvements in the power electronics technology enable the affordable nature of the variable-speed drives and offer resurgence to the use of hybrid vehicles.

Among a host of drive motors the switched reluctance motor (SRM), owing to its exclusive features such as lack of any coil or permanent magnet on the rotor continue to occupy a pre-eminent place. The use of silicon steel in the stator winding allows recycling and ensures a higher reliability for the operation of SRM in hard or sensitive conditions [2]-[4]. Besides the salient rotor structure produces a high torque/inertia ratio to guarantee a fast acceleration and deceleration with low load inertia. Despite the recent developments in the design and application of the SRM [5]-[9], the cost and supply of rare-earth permanent magnets poses a problem for future mass production.

The reports reveal that the SRM can be designed to be competitive with permanent magnet brushless dc motors from the standpoint of efficiency [10]. The use of 6.5% Si steel with 0.10 mm thickness for the core material appears to be the primary reason for enabling the loss reduction and achieving a higher efficiency. It thus becomes important to use proper electrical steel sheets as material for the core [11] and gathers merit to predict the motor core loss reliably. It turns out to be imperative for estimating the dependence of the motor core loss on the typical magnetic properties in terms of the choice of the core material.

The magnetic cores for the low-voltage ac electric motors, drawn from cold rolled non-oriented (CRNO) electrical steel sheets [12]-[13] classify themselves as soft ferromagnetic materials produced from Fe-Si-C alloys. The cold rolled non oriented electrical steel sheets with nearly isotropic magnetic properties enjoy restricted silicon levels to about 3-3.5% due to rolling behavior [12]. The issue of the core losses prediction in CRNO steel sheets invites attention for the designers of magnetic cores [14].

The influence of lamination material on the performance of a single-phase induction motor under sinusoidal waveform excitation [15] and an inverter-driven three-phase induction motor [16] have been investigated by Honda et al. and found that optimum Si content and the other associated material conditions change in accordance with the design considerations such as the stator flux density and the rotating speed. The new magnetic parameters, closely correlated with the 1.5T core loss and 1.0T permeability have been reported by Blazek et al. to be effective for predicting the motor efficiency of single-phase and three-phase induction motors [17].

The design of a SRM with a rotor consisting of two hollow iron cylinders and a stator excited in a way that allows a one directional current flow to minimize the core losses has been discussed in [18]. The core losses and efficiency of the SRM in continuous current mode of operation has been predicted using analytical technique by Amir Parsapour et al. [19]. The core losses have been computed in different parts of the SRM using FEM (Finite Element Method) and Transient-FEM in [20]-[21] respectively. The effect of dynamic eccentricity (DE) and static eccentricity (SE) on the power losses of the induction machines has been examined using PWM voltage control by 2D-FEM [22].

In spite of the study, still it calls for efforts to reduce the core losses of the electric motors in a perspective to improve its magnetic circuit performance and assuage a higher operational efficiency. The primary effort extends to examine the choice of proper electrical steel sheets as core material [22] and facilitate to predict the motor core loss reliably at the design stage. The key feature corners to reduce the core loss of the motor and allow it perform to the best of its capability. The procedure involves stages of simulation and experimental validation to foresee a path for enhancing the performance of the motor. The theory relates to the

study of the influence of material magnetic properties on the motor core loss of a 12/8 (12 teeth on stator and 8 teeth on rotor) SRM using various non-oriented steels for the core material.

II. SPECIFICATION AND IRON MATERIAL

2.1 Specification

The exercise relies on building the core loss model based on the SRM lamination shapes and dimensional parameters in Table 1 to investigate the influence of electrical steel sheets on the magnetic characteristics and the core loss. It involves varying the material of iron core (both stator core and rotor core) with the other specifications kept consistent. The motor models tested by experiment as seen from Fig. 8 depend on using the progressive die to manufacture the iron cores by the automatic lamination process.

Table 1 Specification of SRM

Item	Specification	Item	Specification
Power (kW)	1.5	Stator-rotor gap (mm)	0.3
Speed (rpm)	5100	Rotor outer diameter (mm)	70
Torque (N-m)	3.1	Rotor yoke thickness (mm)	8
No. of phases	3	Shaft diameter (mm)	30
No. of stator/rotor poles	12/8	Voltage (V)	72
Stator outer diameter (mm)	120	Stator steel weight(kg)	4.6
Stator yoke thickness (mm)	11	Rotor steel weight (kg)	2.5

2.2. The Laminated Electrical Steel

Cold rolled non-oriented (CRNO) steel is specialty silicon steel with 3.25% silicon, 0.5% aluminum and 0.005% carbon, in which magnetic properties are uniform in all angular directions. It inherits high permeability and low coercivity, which turns into high values of induction when a low field is applied and low magnetic losses.

The factors like high induction and permeability is powerful in reducing the size and weight of the parts consequently increases the efficiency; low magnetic losses reduce the generation of Joule heat and energy consumption thus helps in minimizing energy; and a low coercivity helps in producing less humming sound in machines.

The turn standard Epstein tester is interfaced with the system to measure magnetic permeability and core loss over a wide range of frequencies in induction increments of 0.05T. The excitation and measurement system involves a crystal accurate 16 bit sine wave generator, which provides 25 Hz to 450 Hz and equipped with an amplifier rated at peak values of 40 A and 110 V. The repeatability of the measurement system is certified by the instrument manufacturer at 0.5% for magnetic field measurements and 0.2% for power loss measurements. The accuracy and stability appears to be better than those specified in national and international standards [23]-[25]. The Table 2 shows the electrical and physical properties for the materials M400-50A, DI MAX-M19 and DI MAX-M15.

Table 2 Magnetic and Material Properties of Used Core Material

Material	Thickness (mm)	W15/50Hz (W/kg)	Density (kg/m^3)	Resistivity (μΩ-cm)	Max. Relative Permeability
M400-50A	0.50	4.09	7700	42	5250
DI MAX-M19	0.35	2.72	7650	50	7500
DI MAX-M15	0.35	2.56	7650	50	8000

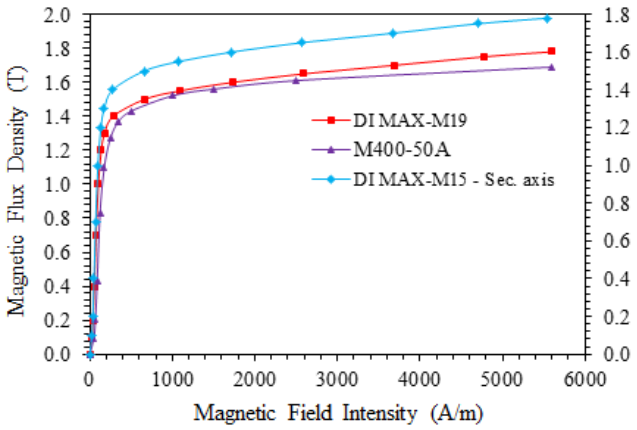

Fig. 1. B-H characteristics of M400-50A, DI MAX-M19 and DI MAX-M15 at 50 Hz.

The Fig. 1 shows the magnetic flux density (B) — magnetic field strength (H) curves of the chosen non oriented steels M400-50A, DI MAX-M19 and DI MAX-M15 as a function of flux swing. Reading from magnetization curves the magnetic field required to attain the magnetic flux density over 1.0 T is 99 A/m in DI MAX-M15, while it is about 105 A/m and 175 A/m in DI MAX-M19 and M400-50A respectively. Especially, the difference in the required magnetic field appears to be larger in the regions of higher magnetic flux density. This is the reason why the motor core loss with using DI MAX-M15 as core material offers a remarkable reduction in the operating condition.

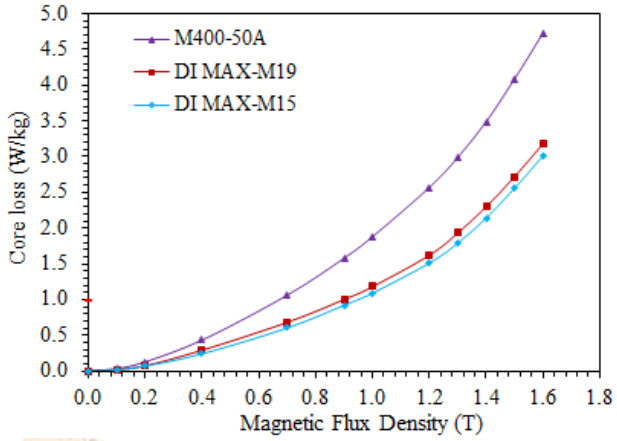

Fig. 2. Core loss curve of M400-50A, DI MAX-M19 and DI MAX-M15 at 50 Hz.

The loss curves of non-oriented steels M400-50A, DI MAX-M19 and DI MAX-M15 drawn at a frequency of 50 Hz seen in Fig.2 and bring out the merits of the loss characteristics of the non-oriented electrical steels. It is evidently shown that the core loss of DI MAX-M15 is lower by 6% of that of DI MAX-M19 and 38% of M400-50A at the frequency of 50 Hz and flux density of 1.5T.

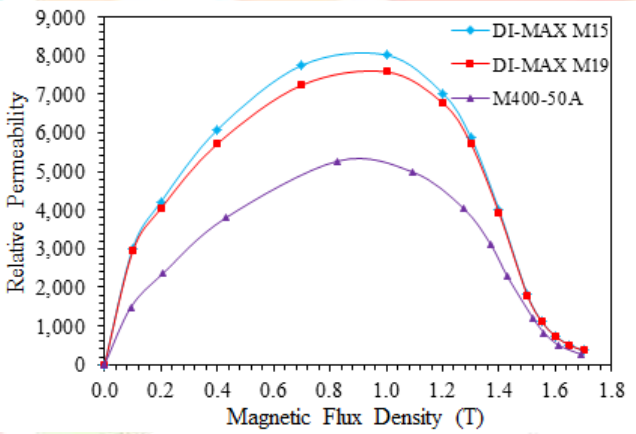

Fig. 3. Relative Permeability of M400-50A, DI MAX-M19 and DI MAX-M15 of at 50Hz.

The relationship between magnetic flux density (B) — magnetic field strength (H) is not linear, as seen from Fig.1 and further allows the relative permeability to vary. The variation of permeability is from (5250 to 8000) at 1.0T and (260 to 360) at 1.7T as indicated in Fig.3. It also shows the flux density at which the relative permeability is maximum and therefrom reveals that DI MAX-M15 steel has a superior relative permeability, far exceeding that of the other non-oriented steels. This property turns out to be essential to enjoy lower losses and in addition these characteristics provide scope for making smaller sized cores.

III. Core Loss Expression and Coefficients

The modeling of the core losses appears to be an enviable task and based on empirical equations obtained from the measurement data. Though a host of methods for determining core losses remain in vogue [26], still the models based on the Steinmetz equation and the loss separation models invite attention and seem to be best suited for fast core losses estimation.
The commonly used model to estimate the core loss and is formulated by means of an empirical equation [26]-[27]

$$W_c = K.f^{\alpha}.B_m^{\beta} \quad (1)$$

Where W_c is the core loss, f the field excitation frequency and B_m the magnitude of magnetic flux density and K, α, β refers to the material parameters. However these material parameters range their validity for a limited frequency and the magnetic flux density [26]-[27]. The modifications to Eq. (1) form part of the contributions in [26] and [28]. The second method of estimating the core losses traces back to the work of Jordan [29] where the core losses separate into hysteresis loss (W_h) and eddy current loss (W_e)

$$W_c = W_h + W_e \quad (2)$$

With α = 1, the hysteresis loss from Eq. (2) can be calculated from Eq. (1) and the eddy current loss from Eq. (2) can be calculated with the help of Maxwell's equations [26]

$$W_e = \frac{\sigma.\pi^2.d^2}{6.\rho}.B_m^2.f^2 \quad (3)$$

Where σ is the conductivity, d is the thickness and ρ is the mass density of steel lamination. The Eq. (3) derived on the homogenous condition of the magnetic material both under consideration of electrical and magnetic conditions [30] follows the assumption of negligible skin effect and the hysteresis losses from Eq. (2) therefore cannot be calculated but requires to be determined by fitting the model to the measurement data.

The third method to improve Eq. (2) is to introduce the excess losses (W_{ex})

$$W_c = W_h + W_e + W_{ex} = K_h f(B_m)^2 + K_e(fB_m)^2 + K_{ex}(fB_m)^{1.5} \quad (4)$$

Where, the coefficients K_h for hysteresis loss, K_e for eddy current loss and K_{ex} for excess loss.

The equation (4) can be written as

$$W_c = K_1 B_m^2 + K_2 B_m^{1.5} \quad (5)$$

From Eq. (4) and (5) K_1 and K_2 can be

$$K_1 = K_h f + K_e f^2 \text{ and } K_2 = K_{ex} f^{1.5} \quad (6)$$

The eddy current loss coefficient is calculated directly as

$$K_e = \pi^2 \sigma \frac{d^2}{6} \quad (7)$$

Minimizing the quadratic form to obtain K_1 and K_2

$$f(K_1, K_2) = \Sigma\left[W_{ci} - \left(K_1 B_{mi}^2 + K_2 B_{mi}^{1.5}\right)\right]^2 = \min \quad (8)$$

where W_{ci} , B_{mi} is the i^{th} point of the data on the measured loss characteristics curve.

The other two loss coefficients are obtained as

$$K_h = \frac{\left(K_1 - K_e f_0^2\right)}{f_0} \text{ and } K_{ex} = \frac{(K_2)}{f_0^{1.5}} \quad (9)$$

Where f_o is the testing frequency for loss curve.

The coefficients K_h and K_{ex} are determined using curve fitting of the core loss data.

Table 3 Core Loss Coefficients

Material	K_h	K_e
M400-50A	2.94×10^{-2}	1.28×10^{-4}
DI MAX-M19	2.08×10^{-2}	6.58×10^{-5}
DI MAX-M15	1.94×10^{-2}	6.52×10^{-5}

The Table 3 includes the values of the coefficients K_h, K_e and K_{ex}, used in the proposed model seen in Eq. (4). The value of K_{ex} is very low for 0.35 mm and 0.50 mm steel sheets, implying that the excess loss is negligible.

IV. Results and Discussion

4.1. Simulation

The effort owes to explore the use of various non-oriented electrical steel for the core and examine its magnetisation characteristics with a perspective to claim an appropriate choice. Among the numerous numerical methods, the FEA is the most frequently used approach for arriving at an appropriate model. The core loss model is used to calculate the losses in stator and rotor core of SRM using FE transient simulation for the chosen three different materials.

The methodology simulates the performance of a 1.5 kW, 12/8 SRM to obtain the machine core loss W_c through the use of Eq. (4) to each element of the finite element mesh. It involves the solution of the Maxwell's equations over each element at each time step and records the values of flux density and thereafter calculates the core losses as a postprocessor step. Since the 2D time-stepping FEM needs more time steps and long computation time, the mesh quality directly affects the accuracy of the calculation. The Table 4 shows the 2D finite element discretization meshes of the stator and rotor finite elements.

Table 4 Discretization Data

Parameter	Value
Number of stator elements	2625
Number of rotor elements	971
Speed	0.025m/s
Calculation time	1h 25m 37s

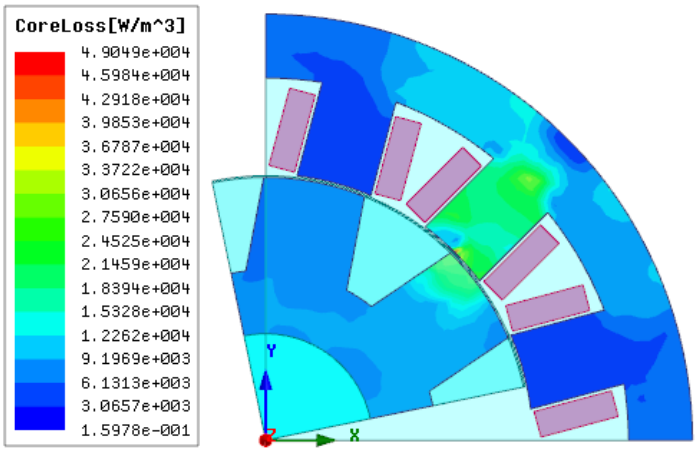

Fig. 4. Core loss distribution of switched reluctance motor using M400-50A at 50 Hz.

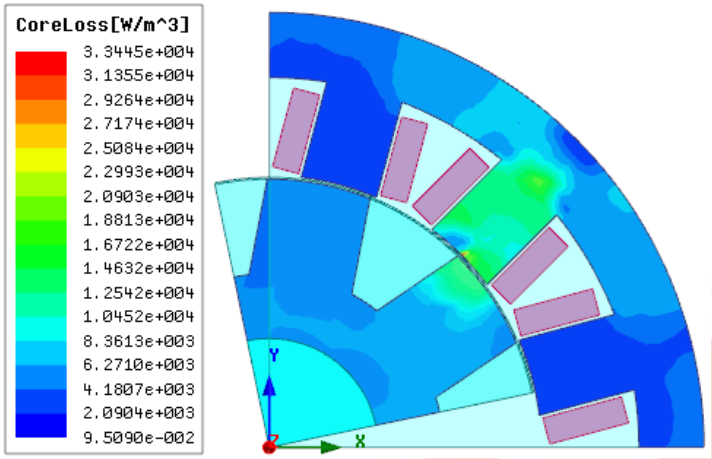

Fig. 5. Core loss distribution of switched reluctance motor using DI MAX-M19 at 50 Hz.

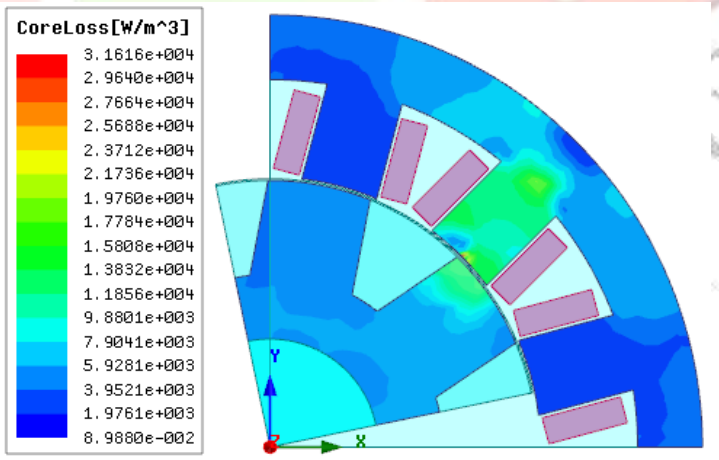

Fig. 6. Core loss distribution of switched reluctance motor using DI MAX-M15 at 50 Hz

.

The Fig.4 – Fig.6 show the core losses in mesh elements in the core of switched reluctance machine and reveals core loss in the stator to be higher than that in the rotor core. It further establishes that the core loss dominates around the corner of the rotor and stator poles. The variation in the losses is due to the occurrence of different flux peaks and the rate of change of flux (dB/dt). The Fig.3 – Fig.6 bring out the influence of relative permeability in terms of decrease in the core loss using M400-50A and DI MAX-M19 with respect to DI MAX-M15 at the operating flux density. The relative permeability in this case goes over 8000 and enables a larger reduction of the core loss in the sense the core loss reduced by 37.4 % and 5.88 % with DI MAX-M15 compared with M400-50A and DI MAX-M19.

The density of steel laminations used in the motor as seen from Table 2. Therefore the maximum core loss employing M400-50A, DI MAX-M19 and DI MAX-M15 are found to be $3.06\times10^{+4}$ W/m^3 (3.97 W/kg), $2.09\times10^{+4}$ W/m^3 (2.73 W/kg) and $1.97\times10^{+4}$ W/m^3 (2.57 W/kg) respectively.

The core loss and steel weight of different sections are determined in the core loss model. The core loss of SRM is

$$W_{cSRM} = \sum W_{ci} \cdot m_i \quad (10)$$

Where W_{ci} and m_i are the core loss and steel weight of various sections respectively. The core loss is 6.92 W for the M400-50A machine, 4.55 W for DI MAX-M19 machine and 4.29 W for DI MAX-M15 machine.

4.2. Experimental Set-Up for Loss Measurement

The Fig.7 shows the fabricated switched reluctance motors using M400-50A, DI MAX-M19 and DI MAX-M15 as a core material. The core metal is subdivided into thin sheets the balance of eddy current path resistance and induced emf shifts so that the overall power wastage in the core is radically reduced. The experimental set-up shown in Fig. 8 includes an induction motor to serve as load machine for controlling the speed, measures the core loss of the SRM.

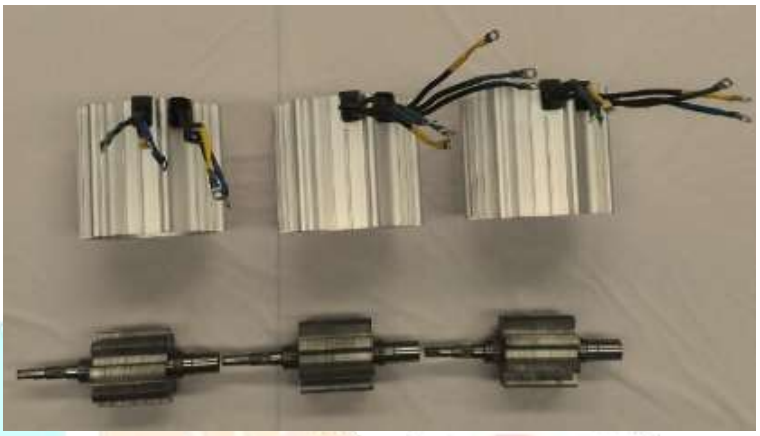

Fig.7. Fabricated SR motors using M400-50A, DI MAX-M19 and DI MAX-M15.

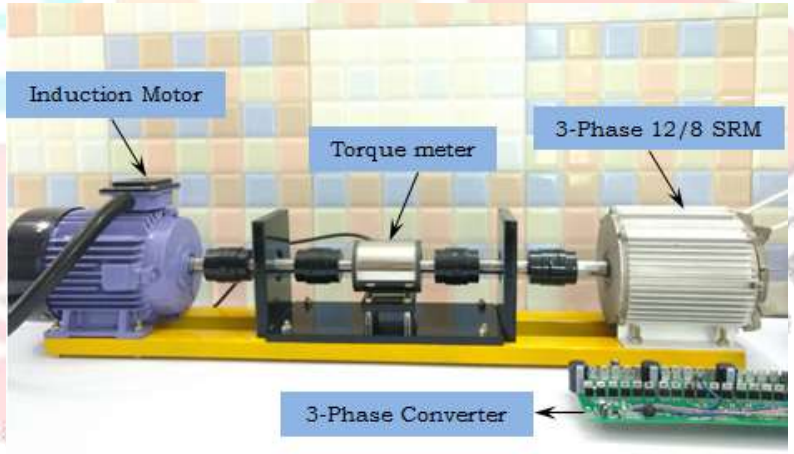

Fig.8. Test bench for measurement of core loss.

The core loss W_{cSRM} in switched reluctance motor is calculated from the shaft output P_{out}, the copper loss W_{cu}, the mechanical loss W_{mech}, and the input electric power P_{in} as

$$W_{cSRM} = P_{in} - P_{out} - W_{cu\_stator} - W_{cu\_rotor} - W_{mech} \quad (11)$$

The electric input power P_{in} of the motor is obtained from the power meter to the motor terminals and the shaft output P_{out} was calculated as the product of the measured torque and the shaft angular velocity.

The copper loss W_{cu_stator} is calculated from the rms current and the winding resistance of each phase. Assuming the winding currents to be I_A, I_B, and I_C so that

$$W_{cu\_stator} = R_A I_A^2 + R_B I_B^2 + R_C I_C^2 \quad (12)$$

The averaged values across the three winding resistances R_A, R_B, and R_C at an ambient temperature for each machine are 0.11 Ω for the M400-50A, 0.058 Ω for the DI MAX-M19 and 0.051 Ω for the DI MAX-M15 machine.

However in SRM the windings present only on stator, therefore

$$W_{cu\_rotor} = 0 \quad (13)$$

The mechanical loss W_{mech} is the product of the rotational angular velocity and the measured torque when the IM drives the shaft with no SRM excitation. The W_{mech} at 2100 r/min was found to be 23.56 W in the M400-50A machine, 17.45 W for the DI MAX-M19 machine and 17.95 W for the DI MAX-M15 machine. The variation is instigated by the differences in coupling alignment and bearing conditions.

Table 5 Comparison of SRMs

Material	Measured Core	Simulated	Measured Copper	Simulated
M400-50A	7.21	6.92	53.24	51.53
DI MAX-M19	4.89	4.55	26.66	25.34
DI MAX-M15	4.72	4.29	23.35	22.57

The Table 5 shows the core loss (W_c) and copper loss (W_{cu}) of the three-phase switched reluctance motor for the different core materials. The observed ratio of core W_c / W_{cu} of about 1:5 to 1:7.5, illustrates the effect of the magnetization behavior of the different core materials.

V. VEHICLE TEST

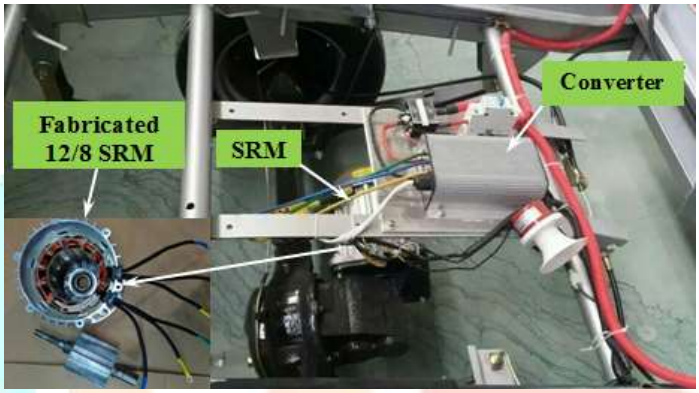

Fig.9. Fabricated SRM in Electrical Vehicle.

The DI MAX-M15 non-oriented electrical steel based 12/8 SRM be-hives to form part of a 72V battery-operated electrical vehicle (EV) as seen from Fig.9. The specifications include a full load and no load speed of motor to be 5100 and 10000 rpm respectively. It bestows to develop lower core and copper losses at a speed in accordance with its inherent characteristics in order to support the requirement of the EV. The design details fall to suit a maximum winding operating temperature below 180ºC and allow the SRM to serve as a reversible drive with forward and braking modes.

VI. CONCLUSION

The effect of non-oriented electric steel for the stator and rotor core of the SRM has been examined through both 2D-FEM simulation and using related experimental study. A loss model has been developed and the coefficients for the various terms predicted. The analytical expressions have been used to compute the losses and the results verified by experiments. The material DI MAX-M15 has been borne to offer a lower core loss for the SRM and seen to adapt well with the change of motor core losses. The investigations have been portrayed to bring out the suitability of DI MAX-M15 as the core material and claim a better performance for the SRM. The results have been belied to explore fresh dimensions for the use of SRM in the utility world.

REFERENCES

[1] International Energy Agency website, 2013. [Online]. Available: http://www.iea.org/etp/tracking/.
[2] Miller, T.J.E. 1993. Switched Reluctance Motors and Their Control. Clarendon, U. K.
[3] Hasanien, H.M. Muyeen, S.M. and Tamura, J. 2010. Torque ripple minimization of axial laminations switched reluctance motor provided with digital lead controller. Energy Convers. Manage., 51: 2402–2406.
[4] Materu, P.N. and Krishnan, R. 1989. Steady-state analysis of the variable-speed switched-reluctance motor drive. IEEE Trans. Ind. Electron., 36(4): 523–529.
[5] Ha, K. and Krishnan, R. 2007. Design and development of low-cost and high efficiency variable-speed drive system with switched reluctance motor. IEEE Trans. Ind. Appl., 43(3): 703-713.
[6] Fuengwarodsakul, N.H. Bauer, S. Tsafak, O. and Doncker, R.W.D. 2005. Characteristic measurement system for automotive class switched reluctance machines. Proceedings in European Conference on Power Electronics and Applications, 44–51.
[7] Nakamura, K. Ono, T. Goto, H. Watanabe, T. and Ichinokura, O. 2005. Nobel switched reluctance motor with wound-cores put on stator and rotor poles. IEEE Trans. Magn., 41(10): 3919–3921.
[8] Inamura, S. Sakai, T. and Sawa, K. 2003. A temperature rise analysis of switched reluctance motor due to the core and copper loss by FEM. IEEE Trans. Magn., 39(3):1554–1557.

[9] Omekanda, A.M. 2003. A new technique for multi-dimensional performance optimization of switched reluctance motors for vehicle propulsion. IEEE Trans. Ind. Appl., 39(3): 672-676.
[10] Chiba, A. Takano, Y. Takeno, M. Imakawa, T. Hoshi, N. Takemoto, M. and Ogasawara, S. 2011. Torque density and efficiency improvements of a switched reluctance motor without rare-earth material for hybrid vehicles. IEEE Trans. Ind. Appl., 47(3): 1240–1246.
[11] Ishida, M. Shiga, N. Honda, A. Kawano, M. and Komatsubara, M. 2001. Estimation of high-efficiency non-oriented electrical steels in motor core application. Proceedings in 1st Japanese-Australian Joint Seminar on Applications of Electromagnetic Phenomena in Electrical and Mechanical Systems, 251–257.
[12] Beckley, P. 2002. Electrical Steels for Rotating Machines. The Institution of Engineering and Technology, London.
[13] Davies, H.A. Fiorillo, F. Flohrer, S. Guenther, K. Hasegawa, R. Sievert, J. Varga, L. and Yamaguchi, M. 2008. Challenges in optimizing the magnetic properties of bulk soft magnetic materials. J. Magn. Mater., 320: 2411–2422.
[14] Toda, H. Senda, K. Morimoto, S. and Hiratani, T. 2013. Influence of various non-oriented electrical steels on motor efficiency and iron loss in switched reluctance motor. IEEE Trans. Magn., 49(7): 3850–3853.
[15] Ling, Z. Zhou, L. Li, H. Zhu, W. Guo, W. and Wang, J. 2014. The use of electrical steels in single-phase induction machines and the modified iron loss test method. IEEE Trans. Magn., 50(11).
[16] Honda, A. Kawano, M. Ishida, M. Sato, K. and Komatsubara, M. 2000. Efficiency of model induction motor using various non-oriented electrical steels. J. Mater. Sci. Tech., 16: 238–243.
[17] Blazek, K.E. and Riviello, C. 2004. New magnetic parameters to characterize cold-rolled motor lamination steels and predict motor performance. IEEE Trans. Magn., 40(4): 1833–1838.
[18] El-Kharashi, E. 2007. Design and predicting efficiency of highly nonlinear hollow cylinders switched reluctance motor. Energy Convers. Manage., 48: 2261–2275.
[19] Parsapour, A. Dehkordi, B.M. and Moallem, M. 2015. Predicting core losses and efficiency of SRM in continuous current mode of operation using improved analytical technique. J. Magn. Mater., 378: 118–127.
[20] Qiang, Y. Laudensack, C. and Gerling, D. 2011. Loss analysis of a canned switched reluctance machine. International Conference on Electrical Machines and Systems (ICEMS): 1-5.
[21] Li, G.J. Ojeda, J. Hoang, E. Lecrivain, M. and Gabsi, M. 2011. Comparative studies between classical and mutually coupled switched reluctance motors using thermal-electromagnetic analysis for driving cycles. IEEE Trans. Magn., 47(4): 839–847.
[22] Belahcen, A. and Arkkio, A. 2010. Computation of additional losses due to rotor eccentricity in electrical machines. IET Electr. Powe.r Appl., 4(4): 259–266.
[23] BIS 649-97. 1997. Methods of testing steel sheets for magnetic circuits of power electrical apparatus. Bureau of Indian Standards, New Delhi.
[24] ASTM A343-97. 2000. Standard test method for alternating-current magnetic properties of material at power frequencies using wattmeter-ammeter voltmeter method and 25-cm Epstein test frame. American Society for Testing and Materials, West Conshohocken.
[25] IEC 60404-2. 2008. Magnetic materials. Part 2: Methods of measurement of the magnetic properties of electrical steel sheet and strip by means of an Epstein frame. third ed., ICS 20.030.
[26] Krings, A. and Soulard, J. 2010. Overview and Comparison of Iron Loss Models for Electrical Machines. J. Electr. Engg., 10(3): 162-169.
[27] Mühlethaler, J. Biela, J. Kolar, W. and Ecklebe, A. 2012. Core Losses under the dc bias condition based on steinmetz parameters. IEEE Trans. Power. Electron., 27(2): 953-962.
[28] Reinert, J. Brockmeyer, A. and Doncker, R.D. 2001. Calculation of losses in ferro and ferri magnetic materials based on the modified steinmetz equation. IEEE Trans. Ind. Electron., 37(4): 1055–1061.
[29] Jordan, J. 1924. Die ferromagnetischen konstanten für schwache wechselfelder. Elektr. Nach. Techn. 1: 7-29.
[30] Pluta,W.A. 2011. Core loss models in electrical steel sheets with different orientation. Electr. Rev., 87(9b): 37-42.